Review article

Tim Starkey* and Pete Vukusic

Light manipulation principles in biological photonic systems

Abstract: The science of light and colour manipulation continues to generate interest across a range of disciplines, from mainstream biology, across multiple physics-based fields, to optical engineering. Furthermore, the study of light production and manipulation is of significant value to a variety of industrial processes and commercial products. Among the several key methods by which colour is produced in the biological world, this review sets out to describe, in some detail, the specifics of the method involving photonics in animal and plant systems; namely, the mechanism commonly referred to as structural colour generation. Not only has this theme been a very rapidly growing area of physics-based interest, but also it is increasingly clear that the biological world is filled with highly evolved structural designs by which light and colour strongly influence behaviours and ecological functions.

Keywords: structural colour; photonics; multilayer interference; diffraction; biology; butterfly.

──────────
*Corresponding author: Tim Starkey, Natural Photonics Group, School of Physics, University of Exeter, Exeter, EX4 4QL, UK, e-mail: t.starkey@exeter.ac.uk
Pete Vukusic: Natural Photonics Group, School of Physics, University of Exeter, Exeter, EX4 4QL, UK

1 Introduction

Colour production in biological systems may be divided into two principle categories: the first is usually associated with chemical processes such as absorption and luminescence; the second relates entirely to coherent scattering processes that underpin the interaction of light with materials that have periodic variations in refractive index.

Pigmentation is the most common biological means of colour production and is the consequence of the wavelength-selective absorption of light by chromophores, the name given to colour-producing molecules [1]. If white light is incident upon a pigment, the resulting scattered light will have some proportion of the light subtracted from the incident spectrum. The molecular structure of a pigment determines the wavelength band over which it absorbs strongly. Pigmentary colour of a biological species is usually synthesised by their physiological processes, although some animals obtain these absorbing molecules through their diet [2]. Pigments that are synthesised by many insects include melanins, pterins, ommochromes, tetrapyrroles, papiliochromes and quinomes, while carotenoid and flavonoid pigments are generally obtained from their diet [2]. Colours produced using pigments are often relatively broadband and cause relatively low-intensity diffuse angle-independent hues.

Modified chromophore chemistry leads to the inelastic scattering processes that give rise to fluorescent colour emission. The common fluorophore-based emissions observed in biological systems usually comprise near-UV absorption with many examples of emission in the blue and green colour wavelengths. Use of fluorescence emission for signalling has been observed in many animals including parrots, spiders and stomatopods [3–5], whilst the directional control of fluorescence emission by photonic crystals has been studied in Swallowtail butterflies [6].

Chemiluminescence is a less common process for colour production, in which light emission arises from a chemical reaction. In biological systems this process is called bioluminescence [1, 2], a well known example of which is the firefly, a species of the Lampyridae beetle family [7]. These light emitting chemical processes are seen in a broad range of organisms, including fungi, bacteria, fly larve, millipedes and earthworms [8], and many deep sea marine animals [9].

The non-pigment-based pathway to colour production is described in terms of structural colour. This phrase is used to describe the wavelength-selective scattering that arises from the interaction of light with structures that have physical dimensions on the order of the wavelength of light. Coherent scattering produces the vivid optical

effects attributed to these structures. The characteristics of this in biological systems can be: intense reflected narrow-band or broad-band colour [10, 11], metallic appearances [12], angle-dependent (iridescent) appearances [13, 14], directional colour variation [15], low-reflective absorbing [16] or transparent systems [17], and strong polarisation signatures [18].

In this review, we discuss aspects of the fundamental optical processes used in biological systems that have evolved for structural colour production. In addition to describing the existence of structural colour systems across a range of different animal and plant phyla, we will particularly describe coherent optical scattering associated with the scales of the insect order of Lepidoptera.

As a vehicle for this we present a brief overview of photonic crystals and demonstrate the associated coherent scattering principles using the example of a one-dimensional layered structure. We describe the existence of more complex photonic structures in a range of biological phyla, and go on to describe the photonic features associated with the general design of lepidopteran scales. We then present a summary of a range of investigations that have focused specifically on *Morpho* butterfly species. Finally we briefly review the growing field of bioinspired research to which *Morpho* photonics has contributed.

2 Historical perspective

Some of the earliest scientific investigations into the science of structural colour phenomena were made by Hooke and Newton. In his 1665 microscope study *Micrographia,* Hooke remarked on "*All the colours of the Rainb*ow" produced by cleaving seemingly colourless muscoy glass [19]. Hooke suggested that the iridescent colour of a Peacock feather may be due to an "*indefinite number of plain and smooth Plates, heaped up, or incumbent on each other*" [19]. Newton also studied the iridescence of Peacock feathers and remarked that a "*great variety of colours*" are produced when blowing upon a soapy liquid [20].

The early 20th century saw more thorough investigations by Mason, Onslow, Rayleigh and others. Their studies of the colours of bird feathers, butterfly wing-scales and beetle elytra elucidated some of the role played in colour production by structures comprising multiple reflecting layers [21–27]. The different visual appearances of many biological systems were attributed to different specific physical phenomena, namely diffraction, interference and scattering by small particles [28].

The invention, and development, of the electron microscope (EM) in the 1930s and 1940s enabled the investigation of biological and synthetic features having microscale dimensions. The first EM studies reported on the colour-producing structures found within bird feathers, and within the scales of butterflies and beetles [29, 30]. Although limited in the image quality and resolution they offered, elaborate multilayer structures with features smaller than the wavelength of light were identified [31].

One of the first mathematical treatments of the optical properties of films was undertaken by Rayleigh in 1887 [32]. Later, Abelès, in 1949, published a rigorous and useful method to obtain the reflection and transmission of thin films [33]. In 1968, intended for an audience of those interested in biological reflectors, Huxley published a recursive method for calculating the reflection and transmission of regularly spaced non-absorbing multilayer films [34]. His discussion emphasised the optical effects relating to layer thicknesses, wave phase and amplitude. In 1972, Land elucidated Huxley's results in the context of the coloured appearance of many biological systems, describing the structure, function and constituent materials of the optical systems present in a wide variety of animals [35].

Ghiradella et al., in 1972, described the bright ultraviolet reflection from a male *Eurema lisa* butterfly, demonstrating that its structural (UV) colour was derived from a very unusual microstructure that appears tree-like in cross-section. Optical measurements combined with electron micrographs revealed the branches of these tree-like 3D ridges formed multilayer reflecting lamellae that were responsible for its UV-iridescent colour appearance [36]. This was one of the key early examples of a structurally coloured insect system featuring a photonic structure that was rather distinct from the more regular 1D semi-infinite multilayered structures theoretically described by Huxley. Two later studies examining *Callophrys* butterflies in the 1970s, described the diffraction of light from 3D simple-cubic networks of ordered porous elements. These were among the earliest studies of highly ordered biological three-dimensional photonic crystals [37, 38].

Modern research into the optics of biological systems has undergone a great deal of change. Plants and animals are not only being investigated to elicit better understanding of their evolutionary, developmental and biological functions; multidisciplinary research into all aspects of such natural systems is extremely active. Greater emphasis is now placed not only on understanding how these structures manipulate light, but also how technology might learn from or incorporate such complex structures into devices or processes.

3 Principles of coherent scattering

3.1 Photonic crystals

In the late 1980s the modern field of photonic crystals was born, principally following the works of John and of Yablonovitch [39, 40]. These developed the analogy between electrons propagating through solid matter with a periodic potential and photons propagating through a periodic dielectric structure. A photonic crystal, therefore, is a structure with a periodically changing dielectric constant that influences the propagation of electromagnetic radiation. By arranging periodically varying refractive indices in one, two or in all three spatial directions, opportunities arise to bend, slow and tailor the propagation of light [41]. Biological systems contain many different examples of photonic crystals with refractive index periodicities [35, 42, 43]. They not only exist in plain 1D geometries, such as with more simple multilayer systems, but are also found in 2D and 3D arrangements. Such structural designs, and the light and colour to which they give rise, often confer specific visual appearances that underpin particular biological functions.

The theory of photonic crystals is described extensively elsewhere [44]. It is nonetheless useful here, however, to outline the physical consequences of light incident on a 1D photonic crystal, especially in relation to the more traditional treatment of multilayer reflection. To this end, consider the propagation of light in an homogeneous non-periodic medium. By using the reduced Brillouin zone (BZ) representation for this system [45] its dispersion diagram can be simplified to a series of photonic bands, with one band originating from each BZ (see Figure 1A).

If this medium is replaced with a structure comprising periodically changing refractive indices, for instance a 1D system comprising high and low refractive index layers, the original reduced BZ band diagram is distinctly modified. Light incident with a wavelength satisfying the resonant conditions of the system, as dictated by the periodicity and refractive indices of the layers, creates standing waves at two different energies. Their presence results in a region in which electromagnetic radiation incident on the 1D photonic crystal is forbidden from propagating, since the group velocity at the band edge is zero. This region, shown in Figure 1B, is referred to as a photonic band gap (PBG), the size of which is strongly influenced by the constituent refractive indices of the photonic crystal.

3.2 Thin film interference

The most common form of PBG structure in biological systems is the 1D periodicity associated with multilayers. It is found widely in the integument and scales of many insects [35, 42, 43] and fish [46–48]. The photonic band structure relating to simple 1D multilayers can be considered using basic ideas of interference. To illustrate this consider the thin film, shown in Figure 2A, that has thickness d and refractive index (RI) n_2. The incident and exit
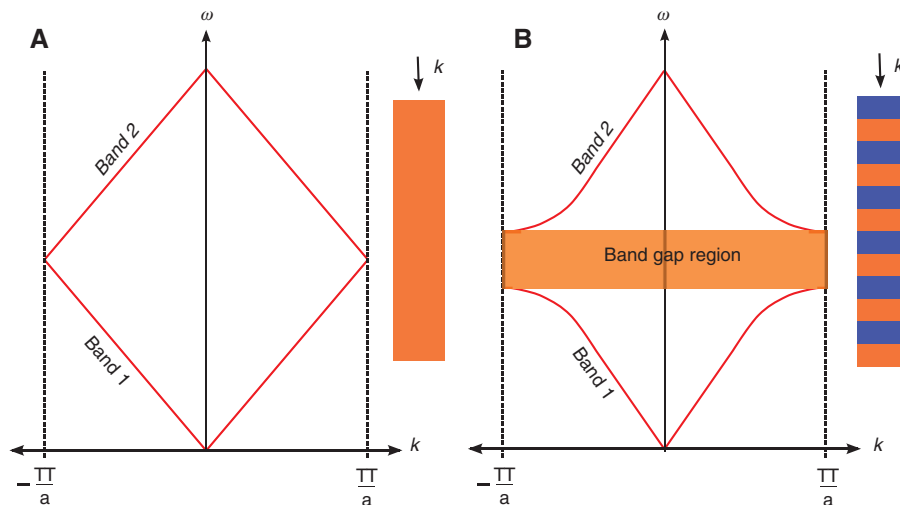

Figure 1 Dispersion diagrams, using the reduced Brillouin zone representation, for: (A) a homogeneous non-dispersive dielectric slab, and (B) a 1D photonic crystal, where ω and k, denote the angular frequency, and wavevector, respectively. (A) and (B) assume a unit cell of periodicity a.
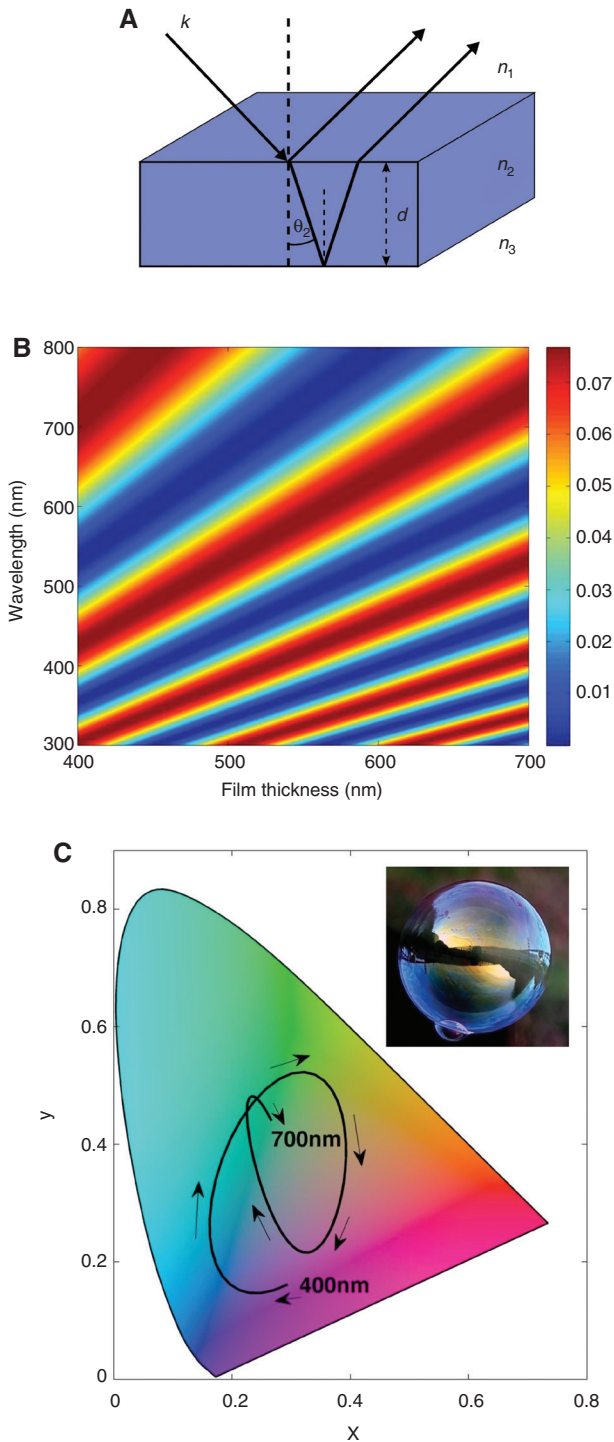
A

B

C

Figure 2 (A) Schematic of interference in a thin dielectric film of thickness d and RI=n_2, (B) reflectance map for a thin dielectric film (representing a soap bubble film) with n_1=n_3=1.00 and n_2=1.33 for film thicknesses ranging from 400 nm to 700 nm, the colour-scale axis represents reflected intensity (indicated in the labelled colour scale bar). (C) CIE colour map, with a CIE-coordinate trace for the film modelled in (B) at normal incidence; black arrowed line represents the way in which normal incidence reflection changes with increase in film thickness, from 400 nm to 700 nm. (Inset: photograph of a typical colour reflection from a soap bubble).

media refractive indices are n_1 and n_3, respectively. Light that enters the film at an angle of θ_2 undergoes a reflection from the top and bottom interface. The optical path difference (*OPD*) between these two reflections is $2dn_2\cos\theta_2$. For constructive interference to occur these reflections should be in phase. The conditions for this are given by:

$$m\lambda = 2n_2 d \cos\theta_2 \text{ for } n_1 < n_2 < n_3$$

$$\left(m + \frac{1}{2}\right)\lambda = 2n_2 d \cos\theta_2 \text{ for } n_1 < n_2 > n_3$$

where m is an integer [49].

To describe wavelength-dependent reflection more accurately, however, the multiple reflections that occur within the film must be considered [50]. The sum of all reflected ray amplitudes is

$$r = r_{12} + t_{12}r_{23}t_{21}e^{-i2\delta} + t_{12}r_{23}^2 r_{21}t_{21}e^{-i4\delta} + t_{12}r_{23}^3 r_{21}^2 t_{21}e^{-i6\delta} + \dots$$

where r_{12} and t_{12} are the Fresnel reflection coefficients at the interface between medium 1 and 2, and the phase difference arising from the film thickness is

$$\delta = \frac{2\pi n_2 d \cos\theta_2}{\lambda}.$$

By summing appropriate amplitudes, the overall reflection coefficient associated with the film's two interfaces is [50]

$$r = \frac{r_{12} + r_{23}e^{-i2\delta}}{1 + r_{23}r_{12}e^{-i2\delta}}.$$

The total reflectance can be calculated using $R=|r|^2$. This can be used to predict the colour reflection of simple structurally coloured systems. As an example, Figure 2B uses this method to illustrate the thickness-dependence of reflectance from a single soap bubble film. Using a CIE colour chart [51], which represents the colour perception associated with human vision, the black line in Figure 2C maps the resulting perceived change in colour appearance of this soap bubble film reflection as film thickness changes.

3.3 Multilayer interference

The most common method for the production of vivid, metallic colours in biological systems is achieved with multiple thin films, or multilayer systems. Here, peak reflectance can be determined using the same geometric considerations as were made for single thin films.

Consider multilayers comprising pairs of thin films; layer 1 has RI equal to n_1 and thickness d_1; layer 2 has RI n_2, and thicknesses d_2. Light is incident at an angle θ_0 from a medium with RI n_0. The condition for constructive interference is now

$$m\lambda = 2(d_1 \sqrt{n_1^2 - n_0^2 \sin^2 \theta_0} + d_2 \sqrt{n_2^2 - n_0^2 \sin^2 \theta_0}\,)$$

where m is an integer. When the optical thickness of both layers is equal, the system is referred to as an *ideal* multilayer [35], and for normal incidence the interference condition reduces to

$$\frac{\lambda}{4} = n_1 d_1 = n_2 d_2$$

Ideal multilayers are a special case, however. Although they are found in some biological examples, such as some fish species' scales [46], the majority of biological multilayers are non-ideal. In these systems the optical thicknesses of layers in each medium can be subject to considerable variability from the ideal multilayer condition, while still exhibiting iridescent colour appearances [52].

A full consideration of wavelength-dependent, polarisation-dependent and angle-dependent reflectance from multilayer systems is commonly performed using transfer matrix methods [50, 53], recursion techniques [54] or iterative approaches [34, 55].

3.4 Factors affecting reflectance in biological systems

Several important variables contribute to the reflection from 1D photonic crystals, or multilayers. In biological systems, these variables can be set or controlled by the animal's or plant's morphology, behaviour or local ecology. The optical effect of, for instance, the number of layers or extent of optical absorption in a system, can be very dramatic, making the difference between a highly reflective and conspicuous insect, or one that is dull and inconspicuous.

3.4.1 Effect of number of layers

The reflectance from a theoretical ideal multilayer, modelled with peak reflectance at 500 nm, is shown in Figure 3A for 3, 9 and 27 layers, and in Figure 3B for much higher layer numbers. The reflectance shows characteristic multilayer spectral features, with a maximum in
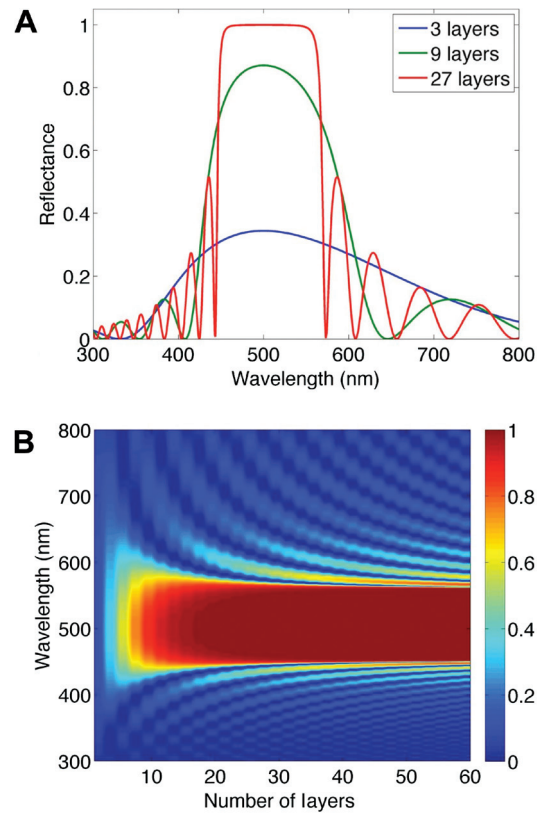

Figure 3 (A) Normal incidence reflectance of an ideal multilayer for 3, 9 and 27 layers, and (B) a reflectance map showing the theoretical variation of normal incidence reflectance with increasing layer number, the colour-scale axis represents reflected intensity (indicated in the labelled colour scale bar). Reflectance was calculated for a multilayer with λ_{peak}=500 nm, n_1=1.40 and n_2=1.00.

reflectance at the peak wavelength and a series of side band minima and maxima.

Using iterative methods, the peak reflectance for an ideal multilayer at normal incidence comprising alternating high RI (n_{high}) and low RI (n_{low}) layers, becomes [55]:

$$R = \frac{\left(\dfrac{n_{high}}{n_{low}}\right)^{2s} n_{high}^2 - n_{inc} n_{out}}{\left(\dfrac{n_{high}}{n_{low}}\right)^{2s} n_{high}^2 + n_{inc} n_{out}}$$

where s denotes the number of high and low RI layer pairs in the system of $2s+1$ layers, and the RI of the incident and exit media are denoted by n_{inc} and n_{out}, respectively. As layer number increases, this reduces to

$$R \cong 1 - \left(\frac{4 n_{inc} n_{out}}{n_{high}^2}\right)\left(\frac{n_{low}}{n_{high}}\right)^{2s}$$

and the peak reflectance rapidly approaches unity. The region of 100% reflectance is the photonic band gap (PBG) described earlier. Figure 3B shows that, with increasing layer number, the peak reflectance increases until it approaches that of a multilayer of infinite layers. The spectral width of a 1D multilayer's PGB is governed by the constituent RIs of the layers [41].

Most structurally coloured biological species have evolved a relatively limited number of layers in their reflecting systems. This is the result of a balance between the relative cost and benefit of layer number with respect to the functions for which each system has evolved. Examples in which biological multilayering comprises 20 layers or more do exist but are rather uncommon [10]. Many examples exist in which fewer than 20 layers are found [52, 56–59]. Species with high layer number tend to display much more intense colour reflections, and if the layers are relatively well aligned, this appears as a metallic-looking reflection due to the specular nature of the bright reflection [60, 61].

3.4.2 Angle-dependence of reflection

The phenomenon of iridescence, namely the change of hue with viewing angle, is a common hallmark of colour produced by periodic structure. Generally, a reflectance maximum will shift to shorter wavelength at larger angles, a property that can be understood using momentum considerations. Light incident normally, that satisfies the resonance condition, has wavevector $k_0 = k_z$. Light incident at some angle, θ, (Figure 4A) will have wavevector $k_0 = k_x + k_z$. To retain the resonant condition, k_z must remain constant, leading to a required increase in k_0. Figure 4B shows the characteristic iridescent reflectance of unpolarised light for a typical ideal multilayer.

In addition to spectral position, the intensity of the peak reflectance band changes with incident angle. For unpolarised light with increasing angle, the reflected intensity decreases to a minimum at the Brewster angle [62]. Beyond this, reflectance increases rapidly. The hierarchical and multi-component nature of biological reflectors often prevents clear discrimination of Brewster reflection features. Some biological examples of Brewster reflection, where multilayer structures are relatively flat and uniform across an area larger than the incident beam spot size, have been described [58, 61]. Certain fish species employ the natural birefringence of their constituent guanine material to inhibit the Brewster effect, and neutralise the associated polarised reflection feature [48].
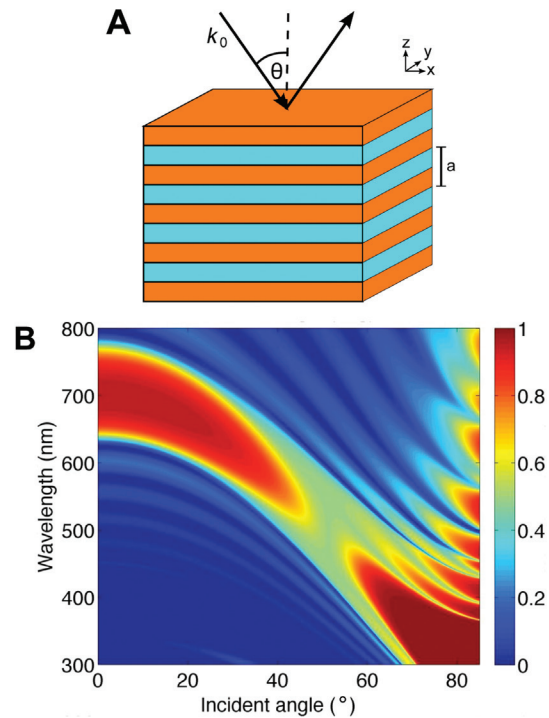
Figure 4 (A) A schematic diagram showing a generic multilayer having light incident with momentum components in the xz-plane, and (B) reflectance map showing the angle-dependence of unpolarised theoretical reflectance from an ideal multilayer with $\lambda_{peak} = 700$ nm at normal incidence, the colour-scale axis represents reflected intensity (indicated in the labelled colour scale bar).

The iridescent, or angle-dependent colour reflection property ascribed to multilayers is inhibited in some animal species: for instance insects with multilayer structures often display bright structural colour that does not change hue with angle. To achieve this they exploit the addition of reflected colour from spatially juxtaposed pointillistic colour-centres to achieve angle independent reflection [63, 64].

3.4.3 Effect of refractive index contrast

The contrast between the high RI, n_{high}, and low RI, n_{low}, causes a pronounced effect on the reflectance. Figure 5 shows the dependence of normal incidence unpolarised reflection on increasing RI contrast, ($n' = n_{high}/n_{low}$) for an ideal 1D 20-layered system using a fixed $n_{low} = 1$. In the absence of absorption as the index contrast increases, both intensity and width of the reflected band increase. For this arrangement, 100% reflectance is achieved when $n' = 1.54$.

The dependence of reflected intensity on n' is a constraining factor for biological systems due to the limited
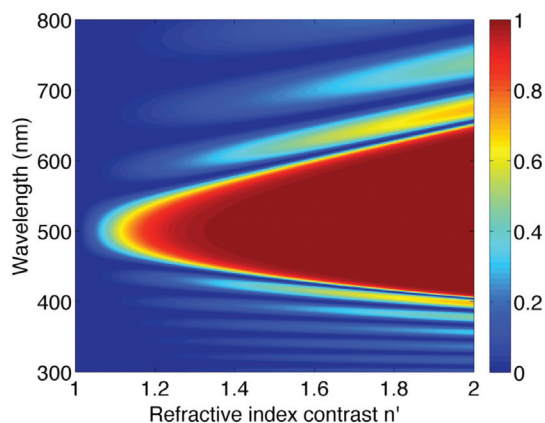
Figure 5 Reflectance map showing the theoretical dependence of normal incidence reflectance on refractive index contrast for a system comprising a 20-layer ideal multilayer, using fixed values λ_{peak}=500 nm and n_{low}=1.00, the colour-scale axis represents reflected intensity (indicated in the labelled colour scale bar).

Table 1 List of published values of refractive indices of materials present in a range of animal and plant biophotonic structures.

Insecta	Cuticle (Lepidoptera)	n_h=1.56 [23, 60], n_l=1.00 (air)
	Cuticle (Coleoptera)	n_h=1.68 (melanin rich) and n_l=1.56 [59]
Aves	Keratin and melanin	n_h=1.69 (melanin) [58], n_l=1.54 (keratin) [65], n_l=1.55–1.57 (keratin) [66]
Fish	Guanine	n_o=1.80 [46], n_o=1.83 and n_e=1.46 [48], n_l=1.33 (water)
Plants	Cellulose	n_h=1.53 (dried) and n_l=1.42 (hydrated) [67]
Phytoplankta	Amorphous silica	n_h=1.46 [68], n_l=1.33 (water)
Crustacea	Carbonates	n_o=1.50 and n_e=1.70 [69], n_l=1.33 (water)
Bacteria	Peptidoglycan	n_h=1.40 [70], n_l=1.33 (water)

High and low RI values are denoted by n_h and n_l respectively. In systems exhibiting birefringence, the ordinary and extraordinary RIs are denoted as n_o and n_e, respectively.

range of materials that are naturally available to animals and plants. While, in technology, photonic systems may be designed and fabricated using a range of high-index materials, including metals and semiconductors, biological processes are limited largely to the use of simple dielectric materials. These rarely have RI values in excess of approximately 1.8, and the systems rarely have RI contrasts in excess of approximately 1.56. The RIs of some common materials found in previously studied bio-optical systems are shown in Table 1.

The materials from which structurally coloured biological systems are fabricated clearly do not prevent the manipulation of light, for instance in the creation of bright coloured reflections. They do, however, limit the extent to which a complete PBG can be established by the structures they form [41].

RI dispersion in several bio-optical materials has been measured experimentally [59, 66, 71].

3.4.4 Effect of optical absorption

Optical absorption in a dielectric medium attenuates light propagating through it according to the Beer-Lambert Law [49]. The absorption-related changes observed in the spectral response of a multilayer depend on whether the absorption is present in the high or low RI layers. When absorption is present in the high RI layers there is a large attenuation of the high-wavelength band-edge, as shown in Figure 6. The opposite is true when absorption is present in the low RI layers. The location-dependent presence of optical absorption therefore, not only can reduce

overall reflected intensity, but it also can shape the spectral response.

The high RI layers in biological systems usually contain light-absorbing pigments. Whilst the real component of RI of many bio-optical tissues have been well characterised, the imaginary component quantifying the absorption is less well known. Melanin is a common absorbing pigment present in insect cuticle, and has very wide spectral absorbance due to its molecular conjugation [72].
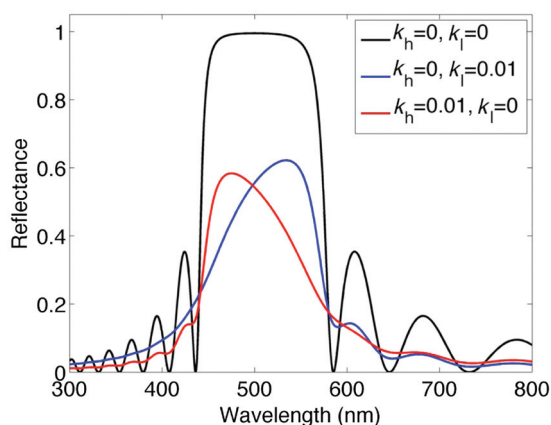

Figure 6 The effect on reflectance at normal incidence of absorption coefficient (k) for an ideal multilayer with λ_{peak}=500 nm. (The imaginary component of the RI in the high and low layers is denoted by k_h and k_l, respectively).

A broadband absorbing pigment, such as melanin, has biological application in photoreceptor shielding, thermoregulation, photoprotection, camouflage, and mechanical strength [72]. It can also be exploited to enhance aspects of colour reflection, for instance in the damselfly *Neurobasis chinensis*, which employs an absorbing layer of melanin below the multilayer reflector as a mechanism to enhance reflected colour saturation [57]. This approach is adopted to varying degrees by a great many animal species [43]. In some species, the absence of melanin in or under a reflecting system desaturates the reflected colour so much that the surface region appears white [73].

One of the first measurements of the complex refractive index of insect cuticle in *Morpho* butterflies found n* $=(1.56\pm0.01)+i(0.06\pm0.01)$ using a fluid immersion technique [60]. Further studies have characterised the wavelength dependence, and concentration-related effects of melanin in biological materials [59, 66].

4 Biological photonic crystals in 2D and 3D

Photonic crystals with 2D and 3D periodicities exist across a range of animal and plant families. Many studies have shown different photonic crystal arrangements, use-strategies and optimisation protocols so that the host system can achieve a specific optical appearance. 2D photonic crystals in biological systems are much less prevalent than those with 3D periodicities and are associated with some avian feathers [74], mammalian eyes [75] and marine creatures [76, 77].

The plumage of male Peacocks contains many differently coloured iridescent feathers. Their colours arise from 2D photonic structures made from arrays of melanin rods connected by keratin within the feather barbules (see Figure 7A and B) [74]. The diverse colours reflected by the different feathers are determined by lattice constant [78]. In another example of a 2D photonic crystal in avian feathers the barbules of black-billed magpies exhibit a structure that has a lattice of holes within a chitin matrix [79].

The iridescent multicoloured cylindrical spines of the polychaete worm, *Pherusa* sp, comprise a 2D photonic crystal that has an optimised hexagonal packing arrangement of hollow cylindrical channels in a chitin medium (see Figure 7C). The hexagonal order is limited to monocrystalline domains of different orientation resulting in an overall polycrystalline effect. The structure is tuned with respect to lattice constant and packing fraction so that
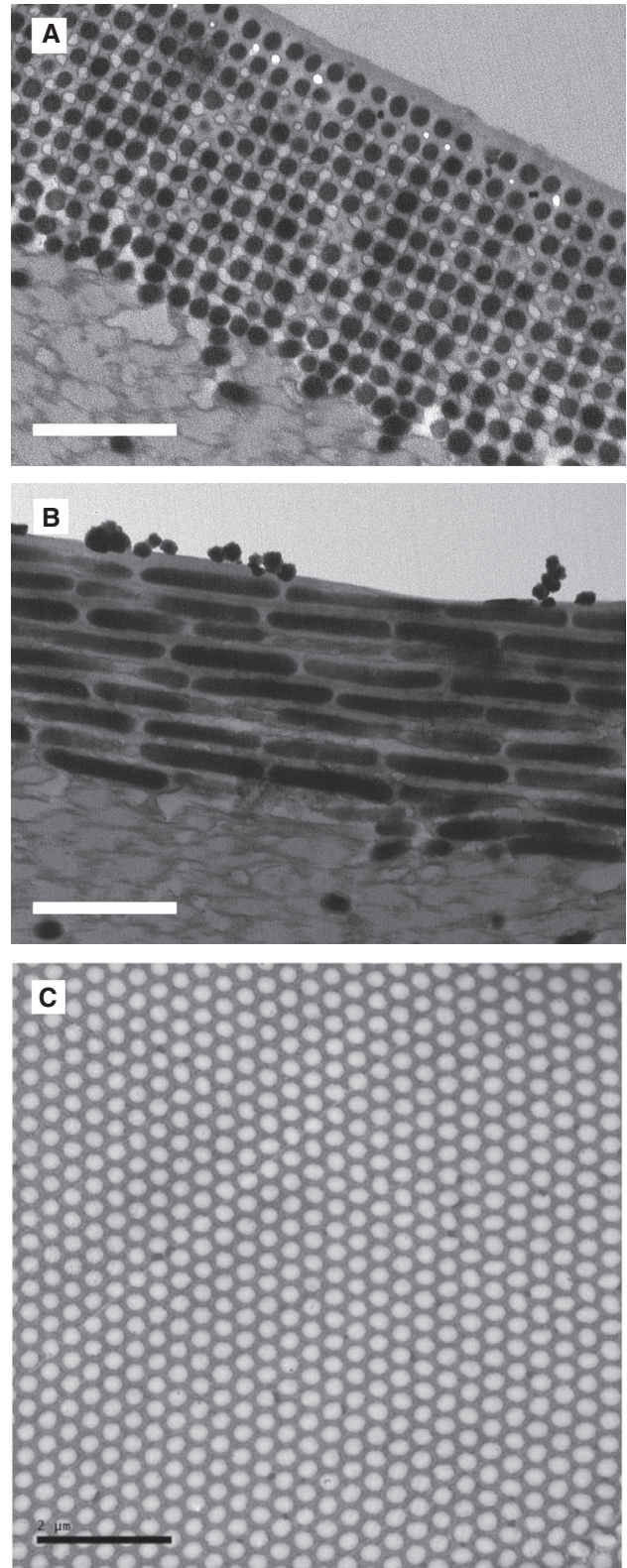

Figure 7 Images of (A) transverse and (B) longitudinal TEM cross-sections of a Peacock feather, with respect to the barbule axis. (C) TEM image of a cross-section of a setae from the polychaete worm Pherusa. (Reprinted from Ref. [77], with permission of APS). Scale bars: (A) and (B) 1 μm; (C) 2 μm.

its response is optimised [77]. The sea mouse, *Aphrodite* sp, also a polychaete worm, contains a similar hexagonal close packed arrangement of channels [76].

3D periodic biological structures are more common than 2D examples. They are present in the scales of many butterflies and beetles and in the feathers of some birds. The way in which these structures are fabricated is not well understood in all cases, but some are believed to use the dynamic self-assembling processes associated with lipid-bilayer interactions [80, 81].

Photonic systems with gyroidal crystal structures are found in Papilionid and Lycaenide butterfly scales. The scales of the *Parides sesostris* butterfly, for instance, contain intra-scale domains of the gyroidal photonic crystal [42] with varying crystal domain orientations, as shown in Figure 8. The pointillistic multicolour contribution of differently oriented domains results in a colour-averaging effect that produces an angle-independent overall green colour [82, 83]. Extensive modelling of the electromagnetic responses of the *P. sesostris* gyroid structure has shown that it has a filling fraction optimised to maximise the reflected bandwidth for light incident normal to the structure [84]. The photonic structures

present in the scales of another butterfly, *Callophrys rubi*, also appear to have an optimised filling fraction [83].

Other biological photonic crystal geometries have been found. The diamond photonic structure is considered a special case due to it being the most isotropic periodic structure of the more commonly encountered crystal classes [85]. The multi-domained photonic crystal in the weevil *Lamprocyphus augustus*, was the first discovered example of this (see Figure 9) [86]. Despite the limited RI contrast between chitin and air that form its system, there is a cumulative PBG at green wavelengths for different crystal planes. The diamond photonic crystal arrangement has also been discovered in the scales of other beetles [87].

Another beetle-based example of photonic crystals demonstrates the contrasting optical properties of highly ordered 3D structures versus quasi-ordered 3D structures. *Eupholus magnificus* exhibits two differently coloured bands (see Figure 10A) across its elytra, one of which is metallic in appearance due to highly specular reflection from ordered structure. The second coloured band is less intense and results from a more diffuse reflection from less ordered structure. Analysis of the associated scales shows that this difference arises from the 3D arrangements of
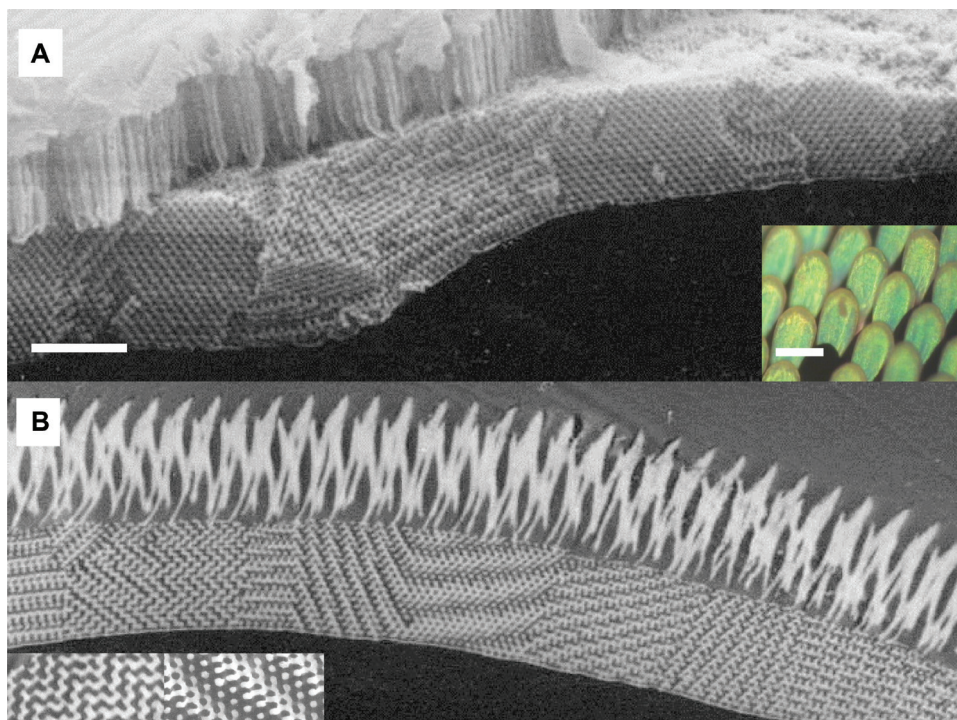

Figure 8 (A) SEM image of a cleaved sectional face of a *P. sesostris* iridescent scale showing the 3D photonic crystal lattice structure. (Inset: optical microscope image of *P. sesostris* green iridescent scales). (B) TEM image of a thin cross-section through the iridescent scale of (A). The range of different tessellation patterns (two of which are inset) are produced by variations in the orientation of the 3D lattice within juxtaposed domains across the scale. Scale bars: (A) 4 μm, (inset 100 μm), and (B) 4 μm (inset 1 μm).
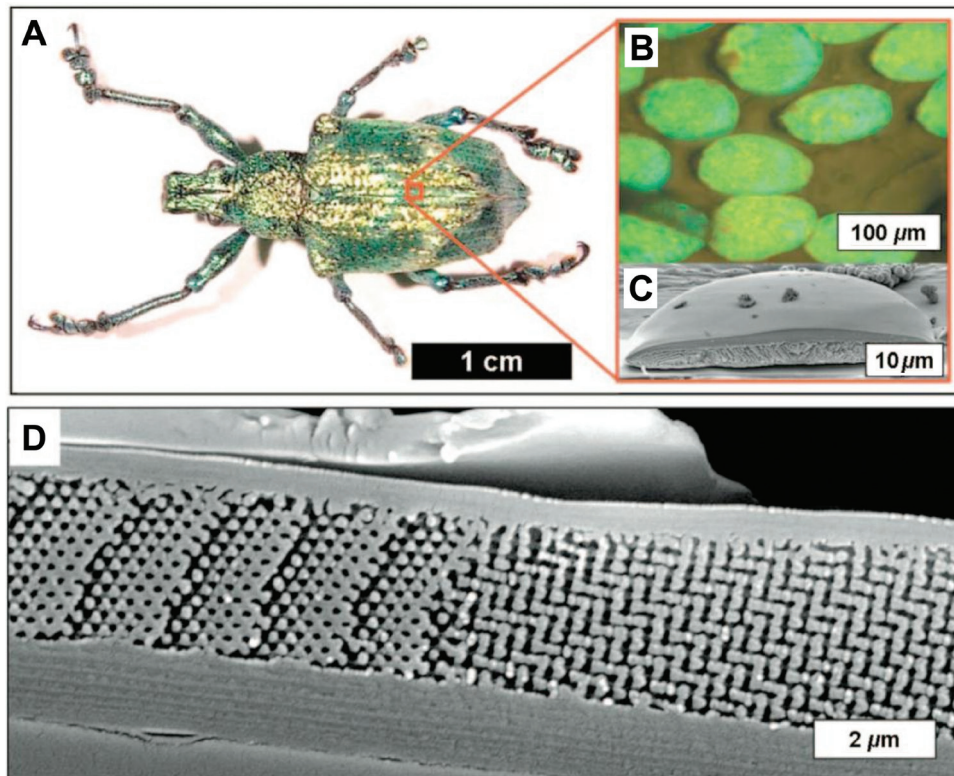
Figure 9 (A) Photograph of the *L. augustus* weevil. (B) Optical micrograph of the green individual scales. (C) and (D) SEM images of a single scale cross-section. (Reprinted from Ref. [86], with permission of APS, and M.H. Bartl.)

cuticle within the scales shown in Figure 10B and C [88]. The coexistence of these two contrasting forms of 3D structural order in the same species is uncommon in biological systems.

5 Iridescent scales in butterflies

Although *Morpho* butterfly photonics will be described in detail, it is useful first to compare their structures to the broad array of other types of photonic systems in Lepidoptera. The structural colour of lepidopteran wings is primarily due to the micro- and nano-structural elements present within their wing-scales. These scales are formed from insect cuticle, which is also used for mechanical functions such as armour and body structure [89, 90]. The morphology of scales is complex. They are formed by the secretion of cuticle from an epithelial cell on the wing substrate, for the formation of a scale, bristle or hair the cell extends a protrusion, shapes it appropriately and secretes cuticle around the entire surface [91]. Details of scale structure and formation are elucidated elsewhere [90, 92–94].

A generic lepidopteran scale has longitudinal ridges that extend down its length. These are often connected by a series of supporting arches, or crossribs. Fine structures, such as lamellae and microribs, can be located on the ridges [90]. Further structures, that are sometimes highly periodic in 2D or 3D, may also be found between the ridges and the lower lamina of the scale.

The scales that are structurally coloured can be broadly classified based on the type and location of the optically reflecting and scattering elements within them. The classification has been loosely divided into three types. Type I scales comprise multilayer structures on the scale ridging. Type II scales have multilayered, or 1D periodic, structure within the scale body. Type III scales have 3D periodic structure within them, or other and more hierarchical pairings of structural designs. Figure 11 schematically represents the basic scale designs and indicates the location on or within the scale of the periodic structure [95]. The scales of the *Morpho* butterfly exhibit Type I scales.

5.1 Overview of colour production in *Morpho* butterflies

The *Morpho* (Lepidoptera: Nymphalidae: Morphinae) is a genus of large tropical butterflies that inhabit lowland
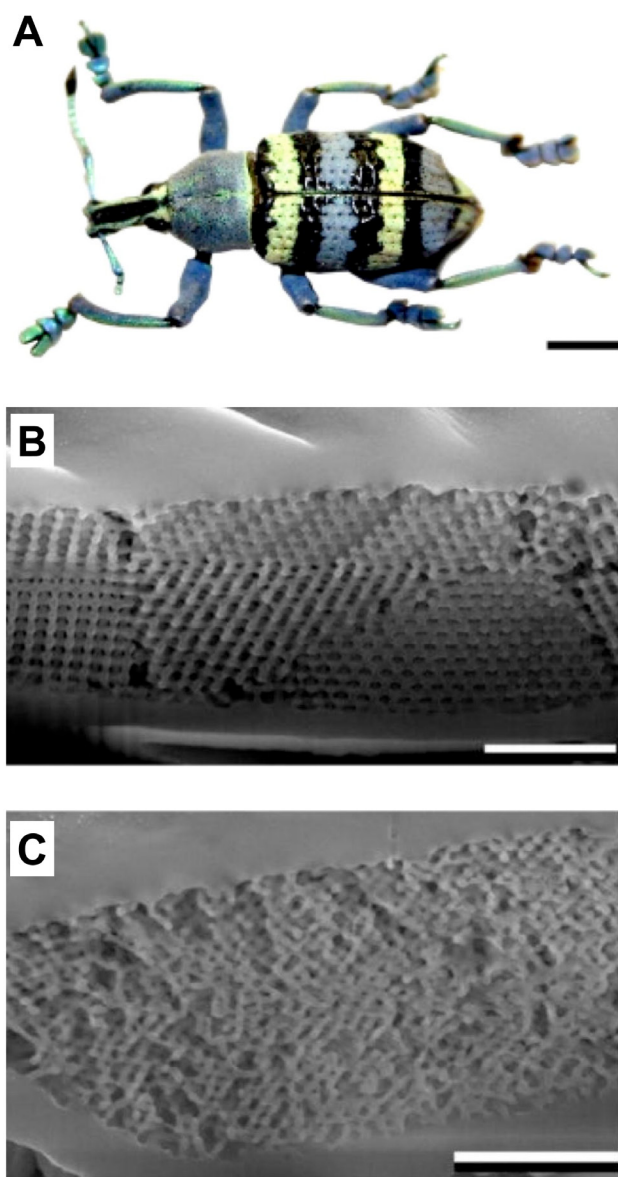
A

B

C

Type I - Ridge lamellae

Generic scale

Type II - Body lamellae

Type III - Body scattering

Figure 11 Schematic illustrations of the classifications of iridescent lepidoteran wing-scale structures. Each scale appears to be a variation on a generic scale structure. (Adapted from Ref. [90], with permission of H. Ghiradella.)

Figure 10 (A) Photograph of *E. magnificus*. SEM images of a fractured: (B) yellow scale, showing the highly periodic 3D lattice, and (C) blue scale, showing the contrasting quasi-ordered structure. Scale bars: (A) 4 mm; (B) and (C) 2 μm. (Reprinted from Ref. [88], with permission of OSA and C. Pouya.)

forest and montane regions of Central and South America [96]. The genus contains many species and subspecies, with some variety in colour appearance and scale type [97]. For the purpose of discussing their visual appearance they can be divided into four groups, namely brownish *Morphos,* bright blue *Morphos*, chalk-white *Morphos*, and gloss-white *Morphos* [96].

The conspicuous appearance of bright blue *Morpho* butterflies (Figure 12A and B) has placed them among the most widely studied and collected butterfly species. The naturalist H.W. Bates remarked upon the dazzling lustre
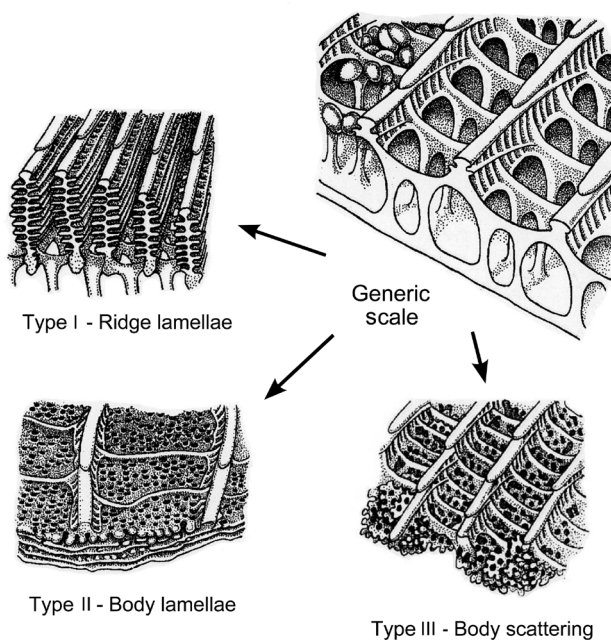
and blue flashes of the *Morpho rhetenor* that could been seen from "*a quarter of a mile off*" [98]. Its bright iridescent colour is believed to enable long-range conspecific communication [99].

Structural colour in bright *Morphos* has been known for over a century. Its dorsal wing surfaces are imbricated with Type I iridescent scales [60]. The ventral wing surfaces often appear dull brown with melanin pigmentation. *Morpho rhetenor* is a well-studied example of a bright blue *Morpho*; its appearance and wing-scale structure are shown in Figure 12.

Since 1999, there has been broad interest in the investigation of the structural colour of *Morpho* butterflies. Before this, most understanding came from observations of Mason and others, on the biological materials present in the scales, and from low quality images obtained through early optical and electron microscopy. More recently, many thorough investigations have used high magnification electron micrographs and rigorous optical measurements, with parallel theoretical analyses, to explain the striking appearance of these insects.

Knowledge that butterfly wing-scales are the colour-centres from which their overall wing appearance arises was developed some time ago. However, such wings are adorned with tens of thousands of scales, many of which overlap partially, are tilted spatially with respect to each
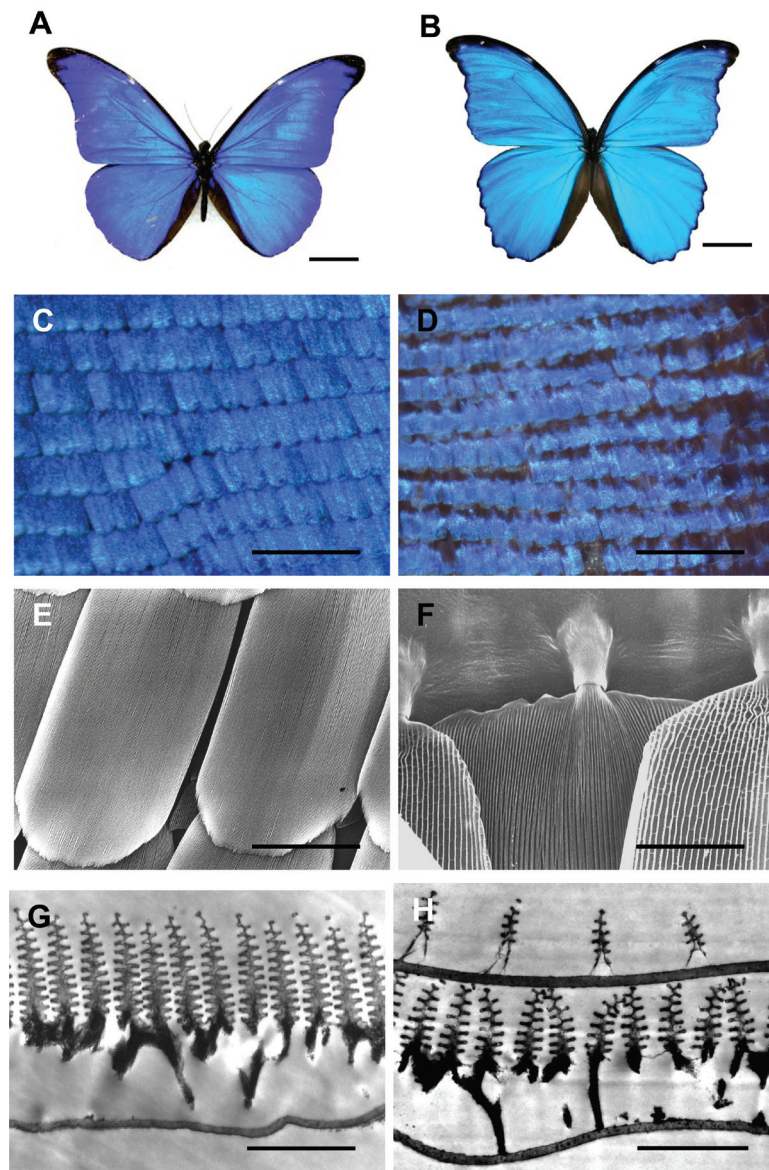
Figure 12 (A) and (B) photographs of *M. rhetenor* and *M. didius*, respectively. (C) Optical microscope image of *M. rhetenor's* imbricated blue iridescent scales. (D) Optical microscope image of *M. didius'* scales with discernible overlayed cover scales. (E) SEM image of *M. rhetenor's* iridescent scale, with visible ridge patterning running down the length of the scale. (F) SEM image of an *M. didius* ground scale, with over-laying cover scales on either side. Also visible are the sockets by which the scales attach to the wing membrane. (G) and (H) TEM cross-sections' through a scale of *M. rhetenor,* and *M. didius*, respectively. (H) shows the cover scale above a ground scale. Scale bars: (A) and (B) 2 cm; (C) and (D) 1 mm; (E) 50 µm; (F) 30 µm; (G) and (H) 2 µm.

other and have inherent small structural variability (see Figure 12C and D). These factors complicate the optical response from the wing and render it difficult to deconvolve and identify the photonic role of individual structural elements from the whole wing. Early experimental optical studies on *Morpho* and other lepidopteran wings comprised recording of reflection spectra from wing samples using large diameter optical beams. More recent studies, however, have led to a significant improvement in understanding these systems by direct optical interrogation of their individual constituent photonic elements.

Single isolated butterfly scales' photonic properties were first described from experimental measurements on two species of *Morpho* butterfly [60]. These two *Morpho* species are bright blue in colour but rather different in their visual appearance: *M. rhetenor* is brilliantly intense and metallic blue in appearance (Figure 12A), whereas *M. didius* reflects a much more diffuse blue colour

(see Figure 12B). Scanning and transmission electron microscopy (SEM and TEM) reveal both *Morphos* exhibit a layer of Type I scales next to their dorsal wing substrate, referred to as ground scales (see Figure 12E–H). *M. didius* also exhibits a second layer of additional near-transparent scales, referred to as cover scales, that completely overlay the ground scales (see Figure 12F).

Absolute angle- and polarisation-resolved measurements of optical reflection and transmission from single scales, detached from *Morphos'* wings, reveal striking differences in the scattering properties of each species' scales. *M. rhetenor's* brightly coloured ground scales reflect 75% of the intensity of incident blue light [60]. This is a remarkably high value considering the factors discussed in Section 2; namely, the relatively low RI contrast of the system's periodic structure, the melanin content of the scales that leads to broadband absorption, the incomplete occupancy of the lamellae and imperfections in the precise periodicity of the structure. Additionally, scattering from individual *M. rhetenor* ground scales is diffusely spread in angle into two broad lobes. *M. didius* ground scales do not show this scattering pattern.

At the whole-wing level the effects of multilayer interference are demonstrated by the reflected blue colour. The individual optical contribution of the cover scale, the ground scale and the wing substrate, however, cannot be separately discerned. An advantage of the single scale measurement approach is that specific scattering mechanisms can be attributed directly to intra wing-scale structures. For instance, strong diffraction can be recorded in transmission through isolated cover scales of *M. didius*. This is not discernable directly from reflection data taken from *M. didius'* wings which themselves are adorned with such cover scales.

These optical observations arise due to the nature of *Morpho* wing-scales' structures. Their cross-sections reveal the discretised multilayer units comprising periodic lamellae of alternating cuticle and air layers (see Figure 12E). An individual multilayer unit exhibits a characteristic tapered shape as well as an asymmetry of lamella positioning around its central stem. This not only reduces the effective multilayer occupancy, but gives rise to its characteristic bi-lobed angle-distribution of optical scatter.

The observed differences between the absolute reflectance of blue light from the ground scales of *M. rhetenor* and *M. didius* are due to the differing number of lamellae present in each species' discretised multilayer unit; there are 9–11 lamellae in *M. rhetenor* (Figure 12G) and 6-8 lamellae in *M. didius* (Figure 12H) [60]. Diffraction by the cover scales of *M. didius* is the underlying reason for the key difference in visual appearance between *M. didius*

and *M. rhetenor*. This creates significantly greater diffuse scattering in reflection for *M. didius*, due to the broader angle-spread associated with diffraction of both incident broadband light and the blue light reflected from the ground scales. This cover scale serves as a selective and isotropic diffuser of blue light in order to distribute reflectance over a wider range of solid angles [100]. The absence of such cover scales in *M. rhetenor* leads to a greater degree of specular reflection and the more metallic blue appearance of the species. Structural irregularity is another contributing factor to the observed wide-angle distribution of light scattered from *Morpho* scales. A simple diffraction model indicates that irregularity in the heights of the ridges within the scale results in its observed wavelength and angle-dependence. The reflected light may be described by an incoherent sum of diffraction arising from the discrete multilayered units [101, 102].

The saturation of the colour appearance of *Morphos* is not solely attributable to structural colour. The localisation of melanin content throughout the ground scales leads to an enhancement of the saturation of blue reflection due to the absorption of complementary wavelengths. This reduces backscatter from the underside of the wing membrane and ventral wing-scales [101]. The contrast in a TEM image of a *Morpho* ground scale generally shows heterogeneous greyscale gradient through the photonic structure [103]. This greyscale contrast strongly implies the presence and extent of melanin content in a scale due to the differential uptake of heavy-metal stains during the TEM sample preparation process [64]. Optical modelling appears to confirm the role and presence of absorbing pigment in these systems [64, 103].

The absence of melanin in what would be an otherwise highly reflective *Morpho* ground scale leads to a significant desaturation of the blue reflection [102]. The bright blue wings of *M. cypris*, for instance, exhibit small regions of wing, in patches and in stripes, which do not contain any melanin. Non-absorbed light that is then scattered between the disordered interfaces of structural components in the dorsal scales, ventral scales and wing substrate in these regions results in their bright white appearance [73]. Other biological structures achieve whiteness through the broadband scattering of light from disordered and pigment-free sub-wavelength structures, some of which are highly optimised for brightness [11, 104, 105].

Penetration of the wing, or an isolated scale, by a wetting fluid such as alcohol, leads to strong modification of the interference conditions. Use of a fluid of RI close to that of water produces a bright green reflection [60]. If the fluid's RI more closely matches that of the cuticle itself, however, then index-matching processes remove

any strong scattered intensity or colour. When a system is fully index matched by a fluid the measurements of light transmitted through it can be used to quantify the absorption arising from the melanin content within the scale [60]. Alternative theoretical approaches, such as the effective medium model, can be employed to fit simulated reflectance to measured reflectance to obtain the complex refractive index of the insect cuticle [106].

The complexity of the *Morpho* structure, comprising discrete units of multilayering and a degree of biological noise in its periodicity, renders it very challenging to model accurately. While straightforward optical multilayer theoretical approaches, described in Section 2, offer a basic means to quantify reflection from *Morpho* scales, they are limited. More sophisticated modelling approaches, which are able to cater for such hierarchical periodicities and multi-dimensional structures, are required to meet the challenge of describing and understanding these systems more accurately. The more successful of these approaches include finite-element method (FEM) modelling [107] and finite-difference time-domain (FDTD) techniques [108]. They both involve the schematic representation, in either 2D or 3D, of the *Morpho* multilayer reflecting unit or a series of these units, simulating optical illumination at a set angle or polarisation, then solving Maxwell's equations to obtain reflectance and transmittance information.

Simple *Morpho* geometries for use with FDTD techniques usually feature the characteristic discrete tree-like units comprising rectangular dielectric blocks. These are geometrically arranged to mimic the distribution of the lamellae associated with *Morpho* scales. Numerical calculation of the hemispherical scatter from such simplified 2D geometries demonstrates the spectral dependence of the tapering and asymmetry of lamellae within the structures [109–111]. 3D FDTD models can help explore the effect of changing the alignment and offset of lamellae on the luminance and colour of scattered light [112, 113]. It also provides more scope with which to study the variation of a broader set of geometric parameters of more realistic *Morpho*-like structures. Using non-standard-FDTD enables some incorporation of small irregularities in the heights of the discrete multilayer structures relative to one another [114]. The discrete nature of such multilayer units, with some height variation, modifies the angular distribution of reflection and enhances the wide-angle reflection for shorter wavelengths [114]. Once this optical data is calculated, it can be used to generate the bidirectional reflectance distribution function [115] for an idealised the *Morpho* system, for which good experimental data exists [116]. This theory can then lead to remarkable graphical rendering of photo-realistic *Morpho* wings [117].

6 *Morpho*-related bioinspired applications

Nature provides a suite of designs for bioinspired applications. The plant Arctium, commonly known as burdock, inspired one of the best known and commercially realised applications. The hooked tips of the barbs on its seed burrs catch effectively on the loops provided by animal fur or human clothing, thereby acting as a good means for dispersal. The mechanism associated with this adhesiveness led to the design and manufacture of *Velcro*™ [118].

Structurally coloured animals and plants continue to inspire a number of technological and industrial applications. Brilliant whiteness in the thin elytral scales of *Cyphochilus* beetles, achieved at very low material cost, elicits interest in the development of optimised paper coating technology [11, 119]. Biological antireflection protocols, at work in some of the transparent wings and ommatidial eye surfaces of Lepidoptera, form potential templates for improving photovoltaic efficiencies [120, 121]. Advanced fabrication techniques have enabled the manufacture of stretchable iridescent fibres inspired by the design and colour appearance arising from multilayer structures found in certain tropical plant seeds [122].

Interdisciplinary scientific interest in the colour appearance of *Morpho* butterflies appears to have led to advances in several specific applications in areas such as textile, reflectors, cosmetics, and in sensing.

Morphotex®, was the first example of a synthetic bioinspired textile. The iridescent appearance of the cloth is produced by pigment-free fibres comprising a multilayer core structure made of alternating polyester and nylon layers [123]. Control of layer thicknesses in each fibre tunes the fabric colour appearance and the absence of dye renders it extremely colourfast.

The ability finely to control multilayer structure fabrication in more complex geometries enables technological mimicry of the desirable colour appearance exhibited by butterflies such as *Morpho*. Specially tailored layer-by-layer deposition of dielectric material can be used to produce flexible multilayer thin film dielectric reflectors that display remarkable bright and angle-independent reflection similar to that exhibited by *Morphos* [124]. Such reflectors have wide-ranging applications in reflective displays, packaging, and advertising.

Pigment-free cosmetic products rely on structural colour centres as the source of the appearance they generate. Mica-based and silica-based systems incorporating periodic polymer networks are used to generate coherent scattering in photonic cosmetic applications. This basis

Figure 13 Photograph of a model wearing pigment-free photonic cosmetics inspired by structural colour in Lepidoptera. (Image courtesy of L'Oreal.)

of colour generation leads to a different appearance aesthetic compared to that associated with pigment-based cosmetics. The design of these products is closely linked to inspiration from butterflies such as *Morpho* [125], see Figure 13.

Colour reflections from *Morpho* wings exhibit sensitivity to the presence of chemical vapours. This arises largely because of the open access to air-spaces between the lamellae that form its reflecting elements, and the formation of thin layers of adsorbate around these lamellae. In this way, *Morpho* butterflies' photonic structures offer bioinspired protocols for chemical vapour sensing [126]. By measuring change in reflectance upon exposure to low concentrations of different chemicals, the *Morpho* scale structure serves as a natural transducer of the chemical signal. Analysis of reflectance demonstrates sensitive and selective optical response to various low-weight organic vapours including alcohols and water. A schematic of this technique is shown in Figure 14. The colour reflectance response of *Morpho* wings also offers sensitivity to mid-wavelength infrared radiation. Thermally-induced reflectivity changes give rise to detectable visible-range colour shifts [127]. While these are interesting avenues of bioinspired exploitation, they appear to serve no discernable biological function to the animal itself, unlike for example, the humidity-induced colour change observed in *Dynastes hercules* beetles, that is providing new inspiration for humidity sensing applications [128–130].

7 Summary and outlook

Here, we have been reviewing aspects of biological photonics. In doing so, we have elucidated some of the properties of photonic crystals, particularly with respect to
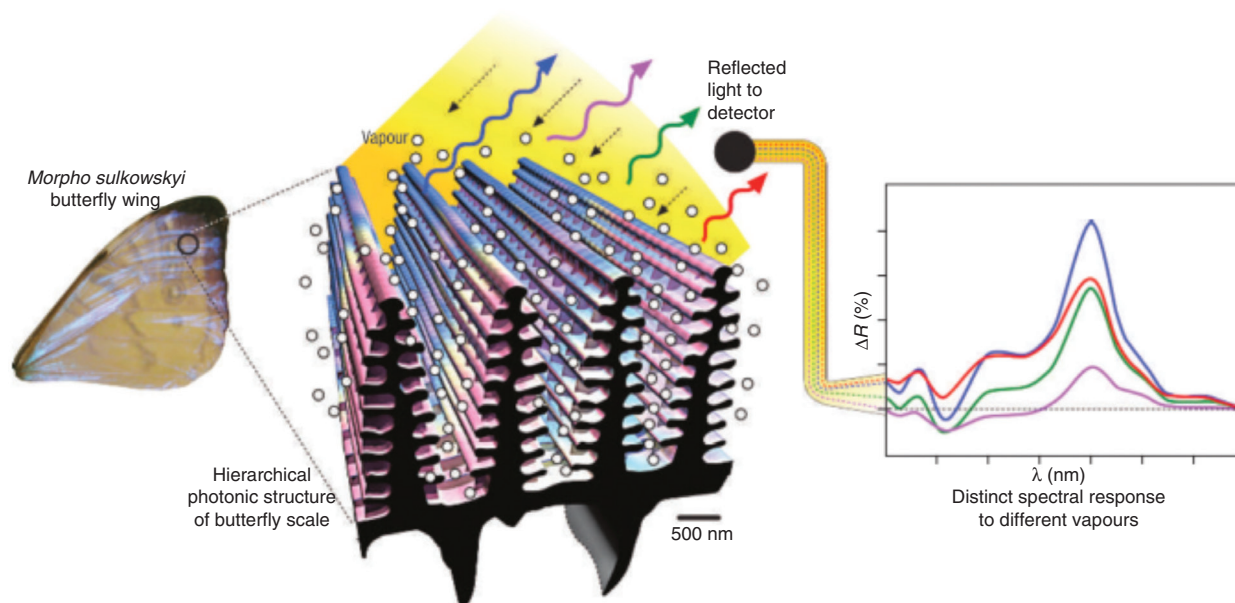
Figure 14 Schematic of the *Morpho*-based vapour sensing principle. Vapour present in the photonic structures of *M. sulkowskyi* iridescent scales measurably changes the differential reflectance spectra ΔR. (Reprinted from Ref. [126], with permission of Macmillan Publishers Ltd: Nature Photonics, and R.A. Potyrailo.)

1D multilayers. We have summarised several key properties of such multilayers, describing the way in which their physical characteristics and material properties can influence their interaction with light. We have summarised the nature of multilayers and some of the higher order periodic structures found in biological systems, principally with respect to insects, and we have particularly focused on presenting more detail on work relating to the *Morpho* butterfly. This is a well-studied species that has a striking structurally coloured bright blue appearance arising from a distinctive and somewhat hierarchical periodic structural origin. Its optical design is one of now many organisms that have inspired technological directions for use and exploitation, and some of these are discussed near the end of this review.

In biological systems, the optical cause and effect that is associated with the capability of periodic structures to manipulate light, thereby giving rise to distinct optical appearances due to tailored colour and polarised light reflection, are now the subject of genuine interdisciplinary scientific interest. Achieving precise understanding of the mechanism with which an exotic-looking animal or plant derives its intense saturated colour, its deep black or brilliant white appearance, or possibly even its dramatic linear or circular polarisation signature, can be an eminently exciting and scientifically rewarding process. From the perspectives of evolutionary diversity, behavioural biology and general zoology, materials science, mainstream optics and photonics, self-assembly chemistry and bioinspired technology, the study of light and colour manipulation in biological systems is yielding rich reward.

Among several ongoing grand challenges in this field, two merit discussion here. Firstly, despite models and descriptions earlier in this review relating to light manipulation and colour generation using precise periodicities in refractive index, it is clear that even the most ordered biological systems are not faultlessly periodic. The extent of variation in the refractive index periodicity of structurally coloured animals and plants has a broad range, from well-ordered to quasi-ordered to genuinely disordered. However, a perfectly periodic biological reflector does not exist. Even in animal examples where it might be argued that the fabrication of very high-quality structural periodicity is approached, or attempted say, there is still a discernable degree of variation. This can be attributed to what might be described as fabrication noise, or in this sense a biological noise, associated with the formation processes.

Some brightly coloured species appear to make use of a significant degree of periodicity variation, often employing quasi-ordered structural geometries. These exhibit the expected optical properties of higher angle-spread and lower intensity in reflection, which contrast to those of species comprising more periodic structural integrity. The fact that some species, for instance *M. rhetenor* described in detail in this review, can tolerate a large degree of variation in the structural periodicity of their reflectors, and can still create an intense and functionally-efficient photonic system, is remarkable. Technological photonics have lessons to learn when it comes to such notable fault tolerance with respect to fabrication of optical reflectors, components and even devices. Further study of the cost and benefit of photonic structure fault tolerance in biological systems will enable cost-saving modifications to the approaches and processes used in technological photonic design and fabrication.

The second challenge for future work relates to gaining a better understanding of the natural processes that lead to the formation of biological photonic systems. Currently, very little is known. Although some self-assembly models and physical processes, for instance those described as being responsible for the formation of gyroidal 3D photonic crystals in some butterflies, provide some insight, there is much left to learn and understand. A photonic engineer of the future could well benefit from the ability to recreate many of these processes in a synthetic environment. At a more fundamental level, little is yet well understood about the genetic information in the sequences of insects, birds, fish and plants that codes for structural colour in their integument, scales, feathers and leaves. Knowledge of this information, and the ability genetically to control or make use of such a structural colour gene, will bring biological photonics science into a very new age.

References

[1] Fox DL. Animal biochromes and structural colours: physical, chemical, distributional and physiological features of coloured bodies in the animal world. Berkeley, CA: University of California Press; 1976.

[2] Vukusic P, Chittka L. Visual signals: color and light production. In: Simpson SJ, Douglas AE, eds. The Insects: Structure and Function. Cambridge: Cambridge University Press; 2013.

[3] Arnold KE, Owens IPF, Marshall NJ. Fluorescent signaling in parrots. Science 2002;295:92.

[4] Mazel CH, Cronin TW, Caldwell RL, Marshall NJ. Fluorescent enhancement of signaling in a Mantis Shrimp. Science 2004;303:51.

[5] Lim MLM, Land MF, Li D. Sex-Specific UV and fluorescence signals in jumping spiders. Science 2007;315:481.

[6] Vukusic P, Hooper I. Directionally controlled fluorescence emission in butterflies. Science 2005;310:1151.

[7] Lall A, Seliger H, Biggley W, Lloyd J. Ecology of colors of firefly bioluminescence. Science 1980;210:560–2.

[8] Wilson T, Hastings J. Bioluminescence: living lights, lights for living. Cambridge, MA: Harvard University Press; 2013.

[9] McCapra F, Hart R. The origins of marine bioluminescence. Nature 1980;286:660–1.

[10] Neville AC, Caveney S. Scarabaeid beetle exocuticle as an optical analogue of cholesteric liquid crystals. Biol Rev 1969;44:531–62.

[11] Vukusic P, Hallam B, Noyes J. Brilliant whiteness in ultrathin beetle scales. Science 2007;315:348.

[12] Parker AR, McKenzie DR, Large MCJ. Multilayer reflectors in animals using green and gold beetles as contrasting examples. J Exp Biol 1998;201:1307–13.

[13] Vukusic P. Now you see it — now you don't. Nature 2001;410:36.

[14] Wickham S, Large MCJ, Poladian L, Jermiin LS. Exaggeration and suppression of iridescence: the evolution of two-dimensional butterfly structural colours. J R Soc Interface 2009;3:99–109.

[15] Vukusic P, Sambles JR, Lawrence CR, Wootton RJ. Limited-view iridescence in the butterfly *Ancyluris meliboeus*. Proc R Soc B 2002;269:7–14.

[16] Vukusic P, Sambles JR, Lawrence CR. Structurally assisted blackness in butterfly scales. Proc R Soc B 2004;271:S237–9.

[17] Stavenga DG, Foletti S, Palasantzas G, Arikawa K. Light on the moth-eye corneal nipple array of butterflies. Proc R Soc B 2006;273:661–7.

[18] Jewell SA, Vukusic P, Roberts NW. Circularly polarized colour reflection from helicoidal structures in the beetle *Plusiotis boucardi*. New J Phys 2007;9:1–10.

[19] Hooke R. Micrographia: or, some physiological descriptions of minute bodies made by magnifying glasses. With observations and inquiries thereupon. London: The Royal Society; 1961.

[20] Newton I. Opticks: or a treatise of the reflection, refractions, inflections and colours. London: W. Innys; 1730.

[21] Mason CW. Structural colors in feathers. I. J Phys Chem 1923;27:201–51.

[22] Mason CW. Structural colors in feathers. II. J Phys Chem 1923;27:401–47.

[23] Mason CW. Structural colors in insects. I. J Phys Chem 1926;30:383–95.

[24] Mason CW. Structural colors in insects. II. J Phys Chem 1927;31:321–54.

[25] Mason CW. Structural colors in insects. III. J Phys Chem 1927;31:1856–72.

[26] Rayleigh L. The iridescent colours of birds and insects. Proc R Soc B 1930;106:618–9.

[27] Mason CW. Transmitted structural blue in microscopic objects. J Phys Chem 1931;35:73–81.

[28] Onslow H. On a periodic structure in many insect scales, and the cause of their iridescent colours. Phil Trans R Soc B 1923;211:1–74.

[29] Frank F, Ruska H. Übermikroskopische Untersuchung der Blaustruktur der Vogelfeder. Naturwissenschaften 1939;27:229–30.

[30] Lippert W, Gentil K. Über Lamellare feinstrukturen bei den schillerschuppen der schmetterlinge vom Urania- und Morpho-typ. Z Morph Ökol Tiere 1959;48:115–22.

[31] Anderson TF, Richards AG. An electron microscope study of some structural colors of insects. J Appl Phys 1942;13:748–58.

[32] Rayleigh L. On the maintenance of vibrations by forces of double frequency and on the propagation of waves through a medium endowed with a periodic structure. Phil Mag 1887;24:145–59.

[33] Abelès F. La détermination de l'indice et de l'épaisseur des couches minces transparentes. J Phys Radium 1950;11:310–4.

[34] Huxley AF. A theoretical treatment of the reflexion of light by multilayer structures. J Exp Biol 1968;48:227–45.

[35] Land MF. The physics and biology of animal reflectors. Prog Biophys Mol Biol 1972;24:75–106.

[36] Ghiradella H, Aneshansley D, Eisner T, Silberglied RE, Hinton HE. Ultraviolet reflection of a male butterfly: interference color caused by thin-layer elaboration of wing scales. Science 1972;178:1214–7.

[37] Morris RB. Iridescence from diffraction structures in the wing scales of *Callophrys rubi*, the Green Hairstreak. J Ent A 1975;49:149–54.

[38] Allyn AC, Downey JC. Diffraction structures in the wing scales of *Callophrys* (*Mitoura*) *siva siva* (Lycaenidae). Bull Allyn Mus 1976;40:1–6.

[39] John S. Strong localization of photons in certain disordered dielectric superlattices. Phys Rev Lett 1987;58:2486–9.

[40] Yablonovitch E. Inhibited spontaneous emission in solid-state physics and electronics. Phys Rev Lett 1987;58:2059–62.

[41] Joannopoulos J, Johnson S, Winn J, Meade R. Photonic crystals: molding the flow of light. Princeton, NJ: Princeton University Press; 2008.

[42] Vukusic P, Sambles JR. Photonic structures in biology. Nature 2003;424:852–5.

[43] Kinoshita S, Yoshioka S. Structural Colors in Biological Systems: Principles and Applications. Osaka: Osaka University Press; 2005.

[44] Joannopoulos JD, Villeneuve PR, Fan S. Photonic crystals. Solid State Commun 1997;102:165–73.

[45] Kittel C. Introduction to Solid State Physics. London: Wiley; 1967.

[46] Denton EJ, Land MF. Mechanism of reflexion in silvery layers of fish and cephalopods. Proc R Soc B 1971;178:43–61.

[47] Levy-Lior A, Shimoni E, Schwartz O, Gavish-Regev E, Oron D, Oxford G, Weiner S, Addadi L. Guanine-based biogenic photonic-crystal arrays in fish and spiders. Adv Funct Mater 2010;20:320–9.

[48] Jordan T, Partridge J, Roberts N. Non-polarizing broadband multilayer reflectors in fish. Nature Photon 2012;6:759–63.

[49] Hecht E. Optics. Reading MA: Addison-Wesley; 2001.

[50] Born M, Wolf E. Principles of Optics. Oxford: Pergamon Press; 1980.

[51] Smith T, Guild J. The C.I.E. colorimetric standards and their use. Trans Opt Soc 1931;33:5–134.

[52] Nixon MR, Orr AG, Vukusic P. Subtle design changes control the difference in colour reflection from the dorsal and ventral wing-membrane surfaces of the damselfly *Matronoides cyaneipennis*. Opt Express 2013;21:1479–88.

[53] Macleod HA. Thin-film Optical Filters. London: The Institute of Physics; 2003.

[54] Amir A, Vukusic P. Elucidating the stop bands of structurally colored systems through recursion. Am J Phys 2013;81:253–7.

[55] Heavens OS. Optical properties of thin films. Rep Prog Phys 1960;23:1–65.

[56] Huxley J. The basis of structural colour variation in two species of *Papilio*. J Ent A 1975;50:9–22.

[57] Vukusic P, Wootton RJ, Sambles JR. Remarkable iridescence in the hindwings of the damselfly *Neurobasis chinensis chinensis* (Linnaeus) (Zygoptera: Calopterygidae). Proc R Soc B 2004;271:595–601.

[58] Stavenga DG, Wilts BD, Leertouwer HL, Hariyama T. Polarized iridescence of the multilayered elytra of the Japanese jewel beetle, *Chrysochroa fulgidissima*. Phil Trans R Soc B 2011;366:709–23.

[59] Yoshioka S, Kinoshita S. Direct determination of the refractive index of natural multilayer systems. Phys Rev E 2011;83:051917–1–7.

[60] Vukusic P, Sambles JR, Lawrence CR, Wootton RJ. Quantified interference and diffraction in single *Morpho* butterfly scales. Proc R Soc B 1999;266:1403–11.

[61] Noyes JA, Vukusic P, Hooper IR. Experimental method for reliably establishing the refractive index of buprestid beetle exocuticle. Opt Express 2007;15:4351–8.

[62] Mahlein HF. Generalized Brewster-angle conditions for quarter-wave multilayers at non-normal incidence. J Opt Soc Am 1973;64:647–53.

[63] Schultz T, Bernard G. Pointillistic mixing of interference colours in cryptic tiger beetles. Nature 1989;337:72–3.

[64] Vukusic P, Sambles R, Lawrence C, Wakely G. Sculpted-multilayer optical effects in two species of *Papilio* butterfly. Appl Opt 2001;40:1116–25.

[65] Shawkey MD, Morehouse NI, Vukusic P. A protean palette: colour materials and mixing in birds and butterflies. J R Soc Interface 2009;6:S221–231.

[66] Leertouwer HL, Wilts BD, Stavenga DG. Refractive index and dispersion of butterfly chitin and bird keratin measured by polarizing interference microscopy. Opt Express 2011;19:24061–6.

[67] Woolley JT. Refractive index of soybean leaf cell walls. Plant Physiol 1975;55:172–4.

[68] Noyes J, Sumper M, Vukusic P. Light manipulation in a marine diatom. J Mater Res 2011;23:3229–35.

[69] Aizenberg J, Tkachenko A, Weiner S, Addadi L, Hendler G. Calcitic microlenses as part of the photoreceptor system in brittlestars. Nature 2001;412:819–22.

[70] Kientz B, Vukusic P, Luke S, Rosenfeld E. Iridescence of a marine bacterium and classification of prokaryotic structural colors. Appl Environ Microbiol 2012;78:2092–9.

[71] Stavenga DG, Leertouwer HL, Hariyama T, De Raedt HA, Wilts BD. Sexual dichromatism of the damselfly *Calopteryx japonica* caused by a melanin-chitin multilayer in the male wing veins. PLoS One 2012;7:e49743.

[72] Riley PA. Melanin. Int J Biochem Cell Biol 1997;29:1235–9.

[73] Yoshioka S, Kinoshita S. Structural or pigmentary? Origin of the distinctive white stripe on the blue wing of a *Morpho* butterfly. Proc R Soc B 2006;273:129–34.

[74] Yoshioka S, Kinoshita S. Effect of macroscopic structure in iridescent color of the peacock feathers. Forma 2002;17:169–81.

[75] Pedler C. The fine structure of the tapetum cellulosum. Exp Eye Res 1963;2:189–95.

[76] Parker AR, McPhedran RC, McKenzie DR, Botten LC, Nicorovici N-AP. Aphrodite's iridescence. Nature 2001;409:36–7.

[77] Trzeciak TM, Vukusic P. Photonic crystal fiber in the polychaete worm *Pherusa* sp. Phys Rev E 2009;80:061908.

[78] Zi J, Yu X, Li Y, Hu X, Xu C, Wang X, Liu X, Fu R. Coloration strategies in peacock feathers. Proc Natl Acad Sci USA 2003;100:12576–8.

[79] Vigneron JP, Colomer J-F, Rassart M, Ingram A, Lousse V. Structural origin of the colored reflections from the black-billed magpie feathers. Phys Rev E 2006;73:021914.

[80] González-Segredo N, Coveney PV. Self-assembly of the gyroid cubic mesophase: lattice-Boltzmann simulations. Europhys Lett 2004;65:795–801.

[81] Saranathan V, Osuji C, Mochrie SGJ, Noh H, Narayanan S, Sandy A, Dufresne ER, Prum RO. Structure, function, and self-assembly of single network gyroid (I4132) photonic crystals in butterfly wing scales. Proc Natl Acad Sci USA 2010;107:11676–81.

[82] Vukusic P, Sambles JR. Shedding light on butterfly wings. Proc SPIE 2001;4438:85–95.

[83] Michielsen K, Stavenga DG. Gyroid cuticular structures in butterfly wing scales: biological photonic crystals. J R Soc Interface 2008;5:85–94.

[84] Pouya C, Vukusic P. Electromagnetic characterization of millimetre-scale replicas of the gyroid photonic crystal found in the butterfly *Parides sesostris*. Interface Focus 2012;2:645–50.

[85] Chan C, Ho K, Soukoulis C. Photonic band gaps in experimentally realizable periodic dielectric structures. Europhys Lett 1991;16:563–8.

[86] Galusha JW, Richey LR, Gardner JS, Cha JN, Bartl MH. Discovery of a diamond-based photonic crystal structure in beetle scales. Phys Rev E 2008;77:050904.

[87] Wilts BD, Michielsen K, De Raedt H, Stavenga DG. Hemispherical Brillouin zone imaging of a diamond-type biological photonic crystal. J R Soc Interface 2012;9:1609–14.

[88] Pouya C, Stavenga DG, Vukusic P. Discovery of ordered and quasi-ordered photonic crystal structures in the scales of the beetle *Eupholus magnificus*. Opt Express 2011;19:11355–64.

[89] Kalmus H. Physiology and ecology of cuticle colour in insects. Nature 1941;148:428–31.

[90] Ghiradella H. Hairs, bristles, and scales. In: Harrison, FW, Locke. M, eds. Microscopic anatomy of invertebrates. New York: Wiley-Liss; 1998.

[91] Ghiradella H. Structure of butterfly scales: patterning in an insect cuticle. Microsc Res Techniq 1994;27:429–38.

[92] Ghiradella H. Structure and development of iridescent lepidopteran scales: the papilionidae as a showcase family. Ann Entomol Soc Am 1985;78:252–64.

[93] Ghiradella H. Structure and development of iridescent butterfly scales: lattices and laminae. J Morphol 1989;202:69–88.

[94] Ghiradella HT, Butler MW. Many variations on a few themes: a broader look at development of iridescent scales (and feathers). J R Soc Interface 2009;6:S243–51.

[95] Vukusic P, Sambles JR, Ghiradella HT. Optical classification of microstructure in butterfly wing-scales. Photon Sci News 2000;6:61–6.

[96] Young AM, Muyshondt A. Geographical and ecological expansion in tropical butterflies of the genus *Morpho* in evolutionary time. Rev Biol Trop 1972;20:231–63.

[97] Berthier S, Charron E, Boulenguez J. Morphological structure and optical properties of the wings of Morphidae. Insect Sci 2006;13:145–57.

[98] Bates HW. The naturalist on the river Amazons. A record of adventures, habitats of animals, sketches of Brazilian and Indian life and aspects of nature under the equator, during eleven years of travel. London: J. Murray; 1863.

[99] Silberglied R. Visual communication and sexual selection among butterflies. In: Vane-Wright RI, Ackery PE, eds. The biology of butterflies. London: Academic Press; 1984.

[100] Yoshioka S, Kinoshita S. Wavelength–selective and anisotropic light–diffusing scale on the wing of the *Morpho* butterfly. Proc R Soc B 2004;271:581–7.

[101] Kinoshita S, Yoshioka S, Kawagoe K. Mechanisms of structural colour in the *Morpho* butterfly: cooperation of regularity and irregularity in an iridescent scale. Proc R Soc B 2002;269:1417–21.

[102] Kinoshita S, Yoshioka S, Fujii Y, Okamoto N. Photophysics of structural color in the *Morpho* Butterflies. Forma 2002;17:103–21.

[103] Mejdoubi A, Andraud C, Berthier S, Lafait J, Boulenguez J, Richalot E. Finite element modeling of the radiative properties of *Morpho* butterfly wing scales. Phys Rev E 2013;87:022705.

[104] Stavenga DG, Stowe S, Siebke K, Zeil J, Arikawa K. Butterfly wing colours: scale beads make white pierid wings brighter. Proc R Soc B 2004;271:1577–84.

[105] Vigneron J, Rassart M, Vértesy Z, Kertész K, Sarrazin M, Biró L, Ertz D, Lousse V. Optical structure and function of the white filamentary hair covering the edelweiss bracts. Phys Rev E 2005;71:011906.

[106] Berthier S, Charron E, Da Silva A. Determination of the cuticle index of the scales of the iridescent butterfly *Morpho menelaus*. Opt Commun 2003;228:349–56.

[107] Dhatt G, Touzot G. The finite element method displayed. Chichester: John Wiley & Sons; 1984.

[108] Yee KS. Numerical solution of initial boundary value problems involving maxwell's equations in isotropic media. IEEE Trans Antennas Propag 1966;14:302–7.

[109] Plattner L. Optical properties of the scales of *Morpho rhetenor* butterflies: theoretical and experimental investigation of the back-scattering of light in the visible spectrum. J R Soc Interface 2004;1:49–59.

[110] Banerjee S, Cole JB, Yatagai T. Colour characterization of a *Morpho* butterfly wing-scale using a high accuracy nonstandard finite-difference time-domain method. Micron 2007;38:97–103.

[111] Steindorfer MA, Schmidt V, Belegratis M, Stadlober B, Krenn JR. Detailed simulation of structural color generation inspired by the *Morpho* butterfly. Opt Express 2012;20:21485–94.

[112] Lee RT, Smith GS. Detailed electromagnetic simulation for the structural color of butterfly wings. Appl Opt 2009;48:4177–90.

[113] Kambe M, Zhu D, Kinoshita S. Origin of retroreflection from a wing of the *Morpho* Butterfly. J Phys Soc Jpn 2011;80:054801.

[114] Zhu D, Kinoshita S, Cai D, Cole J. Investigation of structural colors in Morpho butterflies using the nonstandard-finite-difference-time-domain method: Effects of alternately stacked shelves and ridge density. Phys Rev E 2009;80:051924.

[115] Vukusic P, Stavenga DG. Physical methods for investigating structural colours in biological systems. J R Soc Interface 2009;6:S133–48.

[116] Stavenga DG, Leertouwer HL, Pirih P, Wehling MF. Imaging scatterometry of butterfly wing scales. Opt Express 2009;17:193–202.

[117] Okada N, Zhu D, Cai D, Cole JB, Kambe M, Kinoshita S. Rendering *Morpho* butterflies based on high accuracy nano-optical simulation. J Opt 2012;42:25–36.

[118] Forbes P. The Gecko's Foot: How Scientists are Taking a Leaf from Nature's Book. New York: Harper Perennial; 2006.

[119] Hallam BT, Hiorns AG, Vukusic P. Developing optical efficiency through optimized coating structure: biomimetic inspiration from white beetles. Appl Opt 2009;48:3243–9.

[120] Min W-L, Betancourt AP, Jiang P, Jiang B. Bioinspired broadband antireflection coatings on GaSb. Appl Phys Lett 2008;92:141109.

[121] Boden SA, Bagnall DM. Optimization of moth-eye antire-flection schemes for silicon solar cells. Prog Photovolt: Res Appl 2010;18:195–203.

[122] Kolle M, Lethbridge A, Kreysing M, Baumberg JJ, Aizenberg J, Vukusic P. Bio-Inspired band-gap tunable elastic optical multilayer fibers. Adv Mater 2013:2239–45.

[123] Nose K. Structurally colored fiber "*Morphotex*". Ann High Perf Paper Soc 2005:17–21.

[124] Chung K, Yu S, Heo C-J, Shim JW, Yang S-M, Han MG, Lee HS, Jin Y, Lee SY, Park N, Shin JH. Flexible, angle-independent, structural color reflectors inspired by *Morpho* butterfly wings. Adv Mater 2012;24:2375–9.

[125] L'Oreal. The Secrets of Color. (accessed 26th May 2013 at http://www.loreal.com/research-innovation/push-back-the-boundaries-of-knowledge/the-secrets-of-color.aspx).

[126] Potyrailo RA, Ghiradella H, Vertiatchikh A, Dovidenko K, Cournoyer JR, Olson E. *Morpho* butterfly wing scales demonstrate highly selective vapour response. Nature Photon 2007;1:123–8.

[127] Pris AD, Utturkar Y, Surman C, Morris WG, Vert A, Zalyubovskiy AD, Deng T, Ghiradella HT, Potyrailo RA. Towards high-speed imaging of infrared photons with bio-inspired nanoarchitectures. Nature Photon 2012;6:195–200.

[128] Hinton H, Jarman G. Physiological colour change in the hercules beetle. Nature 1972;238:160–1.

[129] Rassart M, Colomer J-F, Tabarrant T, Vigneron JP. Diffractive hygrochromic effect in the cuticle of the hercules beetle *Dynastes hercules*. New J Phys 2008;10:033014.

[130] Kim JH, Moon JH, Lee S-Y, Park J. Biologically inspired humidity sensor based on three-dimensional photonic crystals. Appl Phys Lett 2010;97:103701.